

# CHARACTERIZATION OF GaInP AVALANCHE TRANSIT TIME DEVICE IN MILLIMETER-WAVE FREQUENCIES

C. C. Meng and G. R. Liao

Department of Electrical Engineering  
National Chung-Hsing University  
Taichung, Taiwan, Republic of China

## ABSTRACT

GaInP material has high breakdown electrical fields and thus is suitable to avalanche transit time device application. Millimeter-wave GaInP IMPATT devices at operating temperature (500K) are analyzed by a large signal model in this paper. The simulation confirms that GaInP IMPATT device has the power density advantage when compared to conventional GaAs and Si IMPATT devices. The improvement in power density is about factor of 4 at 100 GHz. Moreover, GaInP IMPATT devices are easy to incorporate into GaAs millimeter-wave monolithic integrated circuit technology because of the lattice-match and high etching selectivity between GaInP and GaAs materials.

## INTRODUCTION

Utilization of the millimeter-wave region demands a high power monolithic semiconductor source. The recent development of epitaxial techniques such as GSMBE (Gas Source Molecular Beam Epitaxy) and MOCVD (Metal Organic Chemical Vapor Deposition) have made possible the growth of fine epitaxial GaInP layer on GaAs substrate. GaInP is suitable for high power microwave and millimeter-wave active device application because its wider bandgap (1.9 eV) results in high breakdown electrical fields. The high etching selectivity between GaInP and GaAs

has rendered great flexibility and accurate process control in device fabrication. GaInP has been successfully applied to high power GaInP FET device and HBT devices [1], [2]. However, little work has been developed along the direction for IMPATT (IMPact Ionization Avalanche Transit Time) devices. In this paper, a Read type large signal model with the capability of handling ionization rates and saturation velocity as a function of temperature was developed to evaluate GaInP IMPATT devices. GaAs and Si IMPATT devices are also analyzed for comparison purpose. The model developed is very accurate because the calculated results match the state-of-the-art performance for both GaAs and Si IMPATT devices. The simulations reveal that GaInP IMPATT devices have power density advantage over both GaAs and Si IMPATT devices.

## LARGE SIGNAL SIMULATION

GaInP IMPATT devices need to be biased at high breakdown electrical fields and high temperature in millimeter-wave frequencies. A thin avalanche region (down to 0.1  $\mu\text{m}$  for 100 GHz operation) is normally encountered in millimeter-wave IMPATT device operation. Knowledge of accurate impact ionization coefficients for GaInP in the thin avalanche region at high temperature is the first step for large signal simulation. Fu et. al. [3] measured

electron and hole ionization rates of GaInP over moderate and low electrical fields at room temperature by photocurrent multiplication method. Plimmer et. al. has demonstrated that a lucky drift model [4] can accurately describe ionization rates in 0.1  $\mu\text{m}$  avalanche region. Thus, a lucky drift model for ionization rate is used here to extrapolate room temperature ionization rates over moderate electrical fields to high temperature ionization rates over a wide range of electrical fields. The room temperature measured GaInP ionization rates for holes and electrons are fitted into a lucky drift model as shown in figure 1.

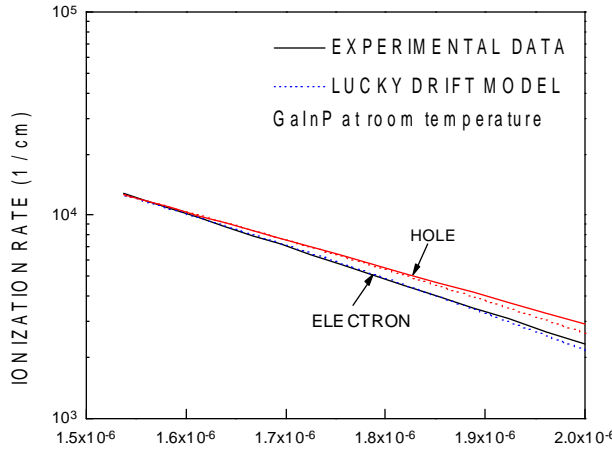


Figure 1. Curve fitting of room temperature GaInP ionization rates by lucky drift model.

A lucky drift model describes ionization rates as a function of electrical fields and temperature by four physical parameters - phonon energy ( $E_p$ ), ionization threshold energy ( $E_T$ ), momentum relaxation length at zero Kevin ( $\lambda_{m0}$ ), and ionization mean free length at zero Kevin ( $\lambda_{ion0}$ ). The fitted physical parameters for GaInP [3], GaAs [5] and Si [6] are shown in table 1. These four physical parameters are independent of electrical fields and have simple temperature dependence. Thus, a lucky drift model can describe ionization rates at high electrical fields

and high temperature in a thin avalanche region.

Table 1. Fitted physical parameters of lucky drift model for GaInP, GaAs and Si.

Material	Carrier	$E_p$ (meV)	$E_T$ (eV)	$\lambda_{m0}$ ( $\text{\AA}$ )	$\lambda_{ion0}$ ( $\text{\AA}$ )
GaInP	Electron	42	2.5	54.8	374
	Hole		1.9	51.5	473
GaAs	Electron	29	1.7	86.4	480.8
	Hole		1.424	73.6	481.8
Si	Electron	55	1.1	95.1	450
	Hole		1.8	89.2	540

A Read type large signal simulation is used to analyze GaInP  $p^+$  $n$  single-drift flat-profile IMPATT devices at operating temperature (500 K). The normalized d.c. current density is set to be 0.1 for all the simulations. A priori knowledge of saturation velocity at operating temperature is not needed in this Read type simulation [7], [8]. Efficiency and power density can be calculated as a function of depletion width as long as the transit time angle is set to be  $\pi$ . The saturation velocity has simple temperature dependence and is proportional to  $[E_p / (2n+1)]^{1/2}$ , where  $n$  is the number of phonons at operating temperature. The room temperature electron saturation velocity is taken as  $10^7$  cm/s for Si,  $7 \times 10^6$  cm/s for GaAs and  $7 \times 10^6$  cm/s for GaInP in the simulation. If a different saturation velocity is assumed, the efficiency is the same for a given depletion width and only a simple calculation for the corresponding frequency is needed.

## RESULTS AND DISCUSSIONS

Figure 2 illustrates the relationship between the efficiency and frequency for GaInP, GaAs and Si  $p^+$  $n$  single-drift flat-profile IMPATT devices at operating temperature. The voltage

amplitude modulation is 50%. The state-of-the-art Si and GaAs  $p^+n$   $p^+n$  single-drift flat-profile IMPATT devices are also shown in figure 2 [9], [10], [11], [12], [13]. The agreements between simulation results and experimental data for GaAs and Si are very good for the frequencies below the efficiency-fall-off corner frequency. A Read type analysis assumes a well-defined avalanche and a well-defined drift region. Thus, a Read type large signal simulation will over-estimate the efficiency for the frequencies where saturation of ionization rates occurs and thus there is no well-defined avalanche region.

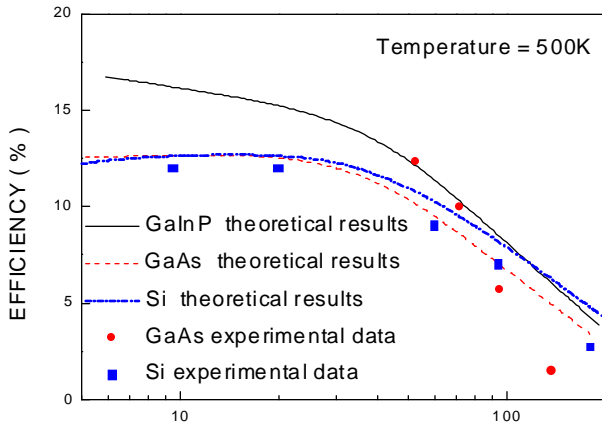


Figure 2. Efficiency as a function of frequency for GaInP, Si, and GaAs  $p^+n$  single-drift flat-profile IMPATT devices at 500 K when  $V_{rf}/V_b=0.5$ .

The normalized admittance values for GaInP  $p^+n$  single-drift flat-profile IMPATT devices with 0.5  $\mu m$  depletion width at 500 K are illustrated in figure 3. The corresponding normalized frequency for GaInP with 0.5  $\mu m$  depletion width is about 50 GHz. There exists a larger conductance for the frequency below the efficiency-fall-off corner frequency as shown in figure 3. However, the susceptance is mostly dominant by the device depletion width capacitance and thus is constant for a given frequency.

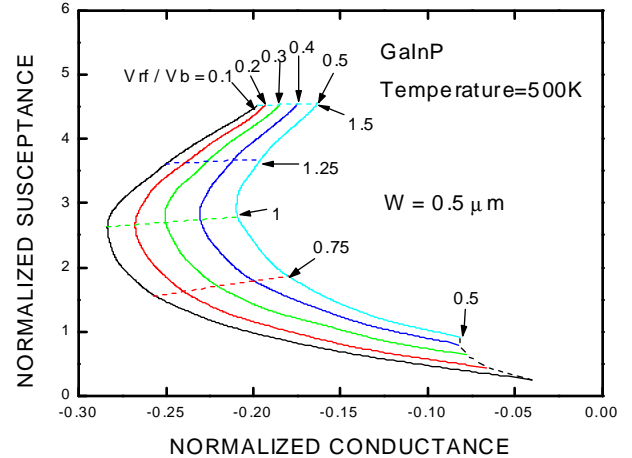


Figure 3. The normalized conductance and susceptance for 50 GHz GaInP  $p^+n$  single-drift flat-profile IMPATT devices at 500 K. Solid arrows point to the normalized r.f. voltage amplitudes and dashed arrows point to the normalized frequencies.

The power density of GaInP, GaAs and Si  $p^+n$  single-drift flat-profile IMPATT devices as a function of frequencies at 500K are shown in figure 4. Figure 4 clearly reveals that GaInP IMPATT devices have the power density advantage than Si and GaAs IMPATT devices because of higher breakdown electrical fields. The power density of GaInP IMPATT device is 4 times higher than that of Si and GaAs IMPATT devices at 100 GHz.

The simulation analyzed millimeter-wave GaInP IMPATT  $p^+n$  single-drift flat-profile structures at operating temperature. A Read type analysis which has a well-defined avalanche region and a well-defined drift region is insufficient to obtain the efficiency for the frequency above the efficiency-fall-off corner frequency. A full scale simulation is thus needed for more accurate result. Nonetheless, a Read type analysis is sufficient to predict at what frequency the efficiency falls off. The efficiency and power density advantage can be still analyzed by a Read type

analysis. The efficiency remains high for the frequencies below 100 GHz frequency for GaInP  $p^+$  n single-drift flat-profile structures. Thus, it is feasible to design a hi-low or low-hi-low Read type structure to further optimize the efficiency by reducing the voltage drop at the avalanche region. The output power and efficiency can be further improved by using a double-drift type design.

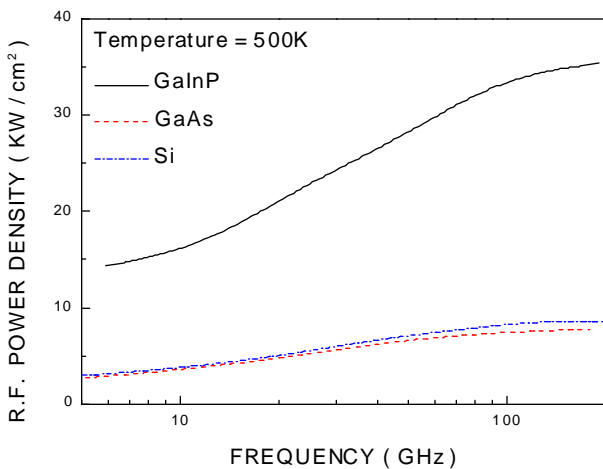


Figure 4 Power density versus frequency for GaInP, Si and GaAs Read diode structure at 500 K.

In conclusion, millimeter-wave GaInP IMPATT devices were analyzed with temperature dependent ionization rates and saturation velocity. GaInP material is attractive to GaAs monolithic integrated circuit technology because of lattice-match property and high etching selectivity between GaInP and GaAs. Our simulation confirms the power density advantage of millimeter-wave GaInP IMPATT oscillators.

#### ACKNOWLEDGMENT

This work was supported by the National Science Council of Republic of China under the contract number NSC 87-2213-E-005-019.

#### References

1. A. W. Hanson, S. A. Stockman, G. E. Stillman, *IEEE Electron Device Lett.*, vol.14, p.25-28, 1993.
2. Y. S. Lin and S. S. Lu, *IEEE Electron Device Lett.*, vol. 16, p.452-454, 1996.
3. S. -L. Fu, T. P. Chin, M. C. Ho, C. W. Tu, and P. M. Asbeck, *Appl. Phys. Lett.*, vol. 66, p.3507, 1995
4. S. A. Plimmer, J. P. R. David, and G. M. Dunn, *IEEE Trans. Electron Dev.* **ED-44**, p.659, 1997, and references therein.
5. Gary E. Bulman, Virginia M. Robbins, and Gregory E. Stillman, *IEEE Trans. Electron Dev.* **ED-32**, p.2454, 1985.
6. W. N. Grant, *Solid-St. Electron.*, vol.16, p. 1189, 1973.
7. C. C. Meng and H. R. Fetterman, *Solid-State Electron.*, vol. 36, p.435, 1993.
8. T. Misawa, *Solid-State Electron.*, vol. 15, p.447, 1972.
9. S. M. Sze, *High-Speed Semiconductor Devices*, Wiley, New York, p.18 and p.555, 1990.
10. X. Zhang, J. Freyer, *Electron. Lett.*, vol. 20, p.359, 1984.
11. H. Eisele and G. I. Haddad, *Electron. Lett.*, vol. 28, p.752, 1992, and references therein.
12. X. Zhang, J. Freyer, *Electron. Lett.*, vol. 20, p.752, 1984.
13. Heribert Eisele, *Solid-State Electron.*, vol. 32, p.253-257, 1989.